NASA/TM—2016-219435

Revisiting of Multiscale Static Analysis of Notched Laminates Using the Generalized Method of Cells

Paria Naghipour Ghezeljeh
Ohio Aerospace Institute, Brook Park, Ohio

Steven M. Arnold and Evan J. Pineda
Glenn Research Center, Cleveland, Ohio

December 2016

NASA STI Program . . . in Profile

Since its founding, NASA has been dedicated to the advancement of aeronautics and space science. The NASA Scientific and Technical Information (STI) Program plays a key part in helping NASA maintain this important role.

The NASA STI Program operates under the auspices of the Agency Chief Information Officer. It collects, organizes, provides for archiving, and disseminates NASA's STI. The NASA STI Program provides access to the NASA Technical Report Server—Registered (NTRS Reg) and NASA Technical Report Server—Public (NTRS) thus providing one of the largest collections of aeronautical and space science STI in the world. Results are published in both non-NASA channels and by NASA in the NASA STI Report Series, which includes the following report types:

- TECHNICAL PUBLICATION. Reports of completed research or a major significant phase of research that present the results of NASA programs and include extensive data or theoretical analysis. Includes compilations of significant scientific and technical data and information deemed to be of continuing reference value. NASA counter-part of peer-reviewed formal professional papers, but has less stringent limitations on manuscript length and extent of graphic presentations.

- TECHNICAL MEMORANDUM. Scientific and technical findings that are preliminary or of specialized interest, e.g., "quick-release" reports, working papers, and bibliographies that contain minimal annotation. Does not contain extensive analysis.

- CONTRACTOR REPORT. Scientific and technical findings by NASA-sponsored contractors and grantees.

- CONFERENCE PUBLICATION. Collected papers from scientific and technical conferences, symposia, seminars, or other meetings sponsored or co-sponsored by NASA.

- SPECIAL PUBLICATION. Scientific, technical, or historical information from NASA programs, projects, and missions, often concerned with subjects having substantial public interest.

- TECHNICAL TRANSLATION. English-language translations of foreign scientific and technical material pertinent to NASA's mission.

For more information about the NASA STI program, see the following:

- Access the NASA STI program home page at http://www.sti.nasa.gov

- E-mail your question to help@sti.nasa.gov

- Fax your question to the NASA STI Information Desk at 757-864-6500

- Telephone the NASA STI Information Desk at 757-864-9658

- Write to:
  NASA STI Program
  Mail Stop 148
  NASA Langley Research Center
  Hampton, VA 23681-2199

NASA/TM—2016-219435

Revisiting of Multiscale Static Analysis of Notched Laminates Using the Generalized Method of Cells

Paria Naghipour Ghezeljeh
Ohio Aerospace Institute, Brook Park, Ohio

Steven M. Arnold and Evan J. Pineda
Glenn Research Center, Cleveland, Ohio

National Aeronautics and
Space Administration

Glenn Research Center
Cleveland, Ohio 44135

December 2016

Level of Review: This material has been technically reviewed by technical management.

Available from

NASA STI Program
Mail Stop 148
NASA Langley Research Center
Hampton, VA 23681-2199

National Technical Information Service
5285 Port Royal Road
Springfield, VA 22161
703-605-6000

This report is available in electronic form at http://www.sti.nasa.gov/ and http://ntrs.nasa.gov/

Revisiting of Multiscale Static Analysis of Notched Laminates Using the Generalized Method of Cells

Paria Naghipour Ghezeljeh
Ohio Aerospace Institute
Brook Park, Ohio 44142

Steven M. Arnold and Evan J. Pineda
National Aeronautics and Space Administration
Glenn Research Center
Cleveland, Ohio 44135

Abstract

Composite material systems generally exhibit a range of behavior on different length scales (from constituent level to macro); therefore, a multiscale framework is beneficial for the design and engineering of these material systems. The complex nature of the observed composite failure during experiments suggests the need for a three-dimensional (3D) multiscale model to attain a reliable prediction. However, the size of a multiscale three-dimensional finite element model can become prohibitively large and computationally costly. Two-dimensional (2D) models are preferred due to computational efficiency, especially if many different configurations have to be analyzed for an in-depth damage tolerance and durability design study. In this study, various 2D and 3D multiscale analyses will be employed to conduct a detailed investigation into the tensile failure of a given multidirectional, notched carbon fiber reinforced polymer laminate. Three-dimensional finite element analysis is typically considered more accurate than a 2D finite element model, as compared with experiments. Nevertheless, in the absence of adequate mesh refinement, large differences may be observed between a 2D and 3D analysis, especially for a shear-dominated layup. This observed difference has not been widely addressed in previous literature and is the main focus of this paper.

Introduction

To accelerate the application of composite structures in aerospace and to reduce the associated certification cost, a robust numerical toolset with an advanced predictive capability is required to assess the damage tolerance and durability of fiber-reinforced composites. To analyze the complex behavior of composite material systems on different length scales (i.e., from the constituent level to the macro or global level) a multiscale framework is beneficial for the design and engineering of these material systems. FEAMAC (Ref. 1) is a synergistic multiscale framework developed by the NASA Glenn Research Center. It couples micromechanics directly to the Abaqus finite element (FE) software package, via Abaqus's UMAT routine, thus enabling the nonlinear analysis of advanced composite structures. In FEAMAC, the generalized method of cells (GMC) (Ref. 1) micromechanics model is called at the desired integration points of the finite element model (Figure 1). It offers both accuracy and efficiency, at the constituent (fiber/matrix) level and at the global level of a composite structural analysis.

The complex nature of the observed composite failure during experiments suggests the need for a 3D multiscale model to attain a reliable prediction, especially when interlaminar damage modes play an important role. However, the size of a multiscale 3D FE model can become prohibitively large and computationally costly. Consequently, 2D models are preferred due to computational efficiency, especially if many different configurations have to be analyzed for an in-depth damage tolerance and durability design study. The available literature data focusing on the differences between 2D and 3D nonlinear FE analysis is unfortunately very sparse (Refs. 2 to 4) and inconsistent. To the authors' knowledge it is even nonexistent in the case of multiscale modeling. Also note that here 2D and 3D refer to the global FE model dimensionality,

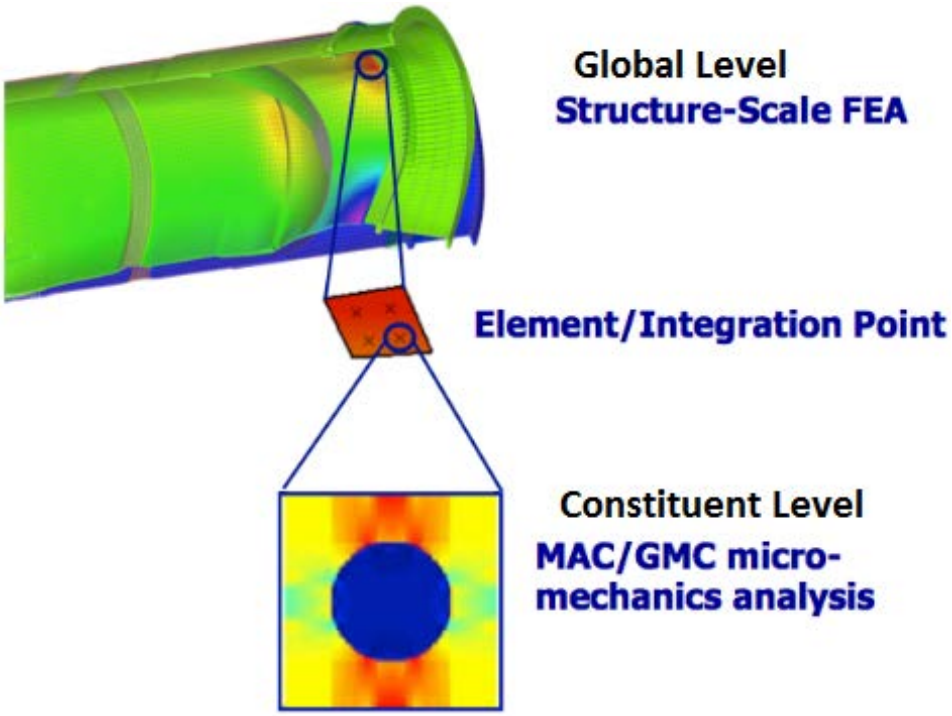

Figure 1.—Implementation of the FEAMAC code within Abaqus built-in UMAT framework.

where a 3D solid model has all six stress components and a 2D shell model has only three (in-plane stress components). The microscale analysis, herein performed by GMC, is always conducted assuming 3D constituent constitutive relationships, albeit with the assumption of double periodicity, which represents continuous fiber reinforcement (Ref. 1).

In a previous study (Ref. 5), blind static failure predictions utilizing FEAMAC were carried out for three different multidirectional open-hole laminates (Layup 1: $[0,45,90,–45]_{2S}$; 2) Layup 2: $[60,0,–60]_{3S}$; 3) Layup 3: $[30,60,90,–30,–60]_{2S}$) as part of the Air Force Research Laboratory (AFRL) (Ref. 5) Tech Scout I project. The aim of this project was to assess the current state of existing multiscale progressive damage prediction methods. During this project, no standardizations for the finite element meshes (i.e., element types, dimensionality, or mesh density) were provided, and the participants were free to model the laminates as they chose. Since a 3D analysis was considered a more realistic representation of experiments (Ref. 4), Naghipour et al. (2016) (Ref. 6) initially decided to simulate the tensile behavior of the composites with a full multiscale 3D analysis, as opposed to 2D FEs at the macroscale. However, subsequent 2D analysis of the same layups incorporating an equivalent mesh density revealed significantly better agreement with experiments (Ref. 6). Consequently, the current study was designed to examine the potential underlying causes of the observed difference between a 2D and 3D analysis, especially for the shear-dominated layup, i.e., Layup 3. (i.e., shear-dominated layups are composed of any given stacking sequence possessing no 0 plies). As such, various 2D and 3D multiscale FEAMAC analyses were employed to conduct a detailed study on all three layups (including Layup 3 which produced the largest error for all Tech Scout participants (Ref. 5)). Based on prior observations (Ref. 6), it was initially assumed that if particular constitutive models were characterized using a macroscopic state of plane stress (2D) and dimensionality consistency was not preserved through the characterization-prediction phase, large differences might be observed between the 2D and 3D multiscale analysis. However, results of the present study suggest that mesh refinement (another form of idealization consistency) plays the greatest role in ensuring accurate predictions in the case of 3D FEA models because through-thickness stresses with very high gradients must be resolved in addition to the in-plane stresses. Detailed findings are reported in this study.

The outline of this paper is as follows: first, a brief overview of the FEAMAC model used in the Tech-Scout I project together with the corresponding results are presented. Current results emphasizing the significance of FE mesh refinement are presented next. Major outcomes and lessons-learned are all summarized in the final section.

Review of Tech-Scout I Project and Results

As mentioned in the introduction, open-hole tension specimens were modeled originally (as part of the Tech-Scout 1 project) using a 3D finite element mesh in order to enable delamination modeling and provide for a more realistic representation of experiments. Each ply of the IM7/977-3, 65 percent fiber volume fraction, composite was discretized using only one single C3D8R (linear 3D) element through thickness. A systematic mesh convergence study was designed and intended to be conducted during the Tech-Scout I project. However, due to the imposed project timeframe only the coarsest mesh (average element size ~2.3 mm in the gage area-Figure 2) was chosen to facilitate timely submission of results. In this study, the originally designed mesh study is implemented, to examine the sensitivity of results with respect to mesh density for both 3D and 2D mesh idealizations. The analyses associated with each Tech Scout layup are repeated with the relatively finer 3D mesh shown in Figure 2 (uniform 1 mm element size in the gage area) to begin with. The FEAMAC multiscale framework was utilized in conjunction with a plasticity theory constitutive model to represent the deformation and damage of the matrix at the microscale and the subcell elimination method for matrix and fiber failure at the microscale (Ref. 1) to predict the tensile failure response of the three notched multidirectional composite laminates (i.e., Layup 1: $[0,45,90,–45]_{2S}$; Layup 2: $[60,0,–60]_{3S}$; and Layup 3: $[30,60,90,–30,–60]_{2S}$). Detailed geometry, boundary conditions, constitutive models and characterization process are discussed in detail in References 5 and 6, and briefly summarized here.

Specimen geometry consists of notched composite laminates with a constant length (138 mm), width (25.4 mm), notch radius (3.375 mm) and varying thickness based on the stacking sequence (Thickness: Layup 1: 2 mm, Layup 2: 2.25 mm, Layup 3: 2.5 mm). As mentioned earlier, a full 3D finite element mesh was used, wherein each ply of the composite is discretized through the thickness using a single C3D8R (linear 3D) element. Displacement boundary conditions were applied at one end of the specimen, while the other end was held fixed in the loading direction (Specimen geometry and boundary conditions are shown in detail in Figure 3). Plasticity-subcell elimination (Plasticity-SE) constitutive model, assigned to every integration point, was calibrated using the unnotched [0], [90], and $[\pm45]_{4s}$ coupon experimental data provided by AFRL through the stand-alone micromechanics analysis code MAC/GMC (Ref. 1). The elastic properties of fiber and matrix (Table 1) were obtained from vendor data or were partially “backed-out” from

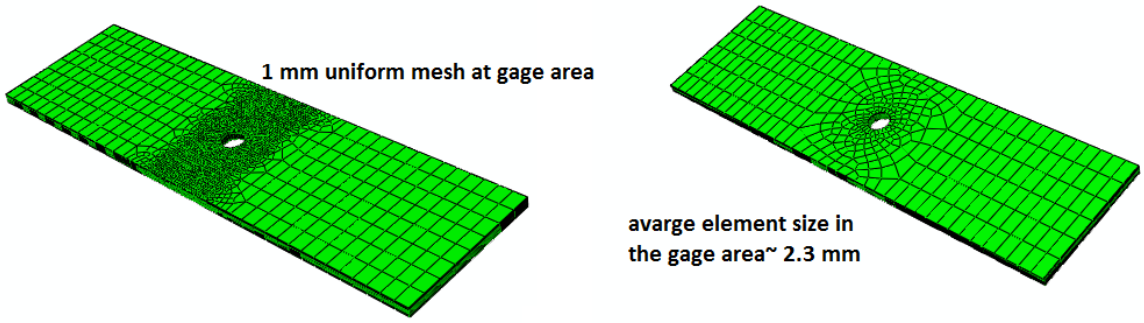

Figure 2.—Finite element meshes used to analyze all three notched layups. Left: element size: 1 mm. Right: Average element size: 2.3 mm.

TABLE 1.—MATRIX (m)/FIBER (f) PROPERTIES AND PLASTICITY-SE THEORY PARAMETERS

E_{f11} = 276 GPa (tension/compression)	$\varepsilon^{ult}_{fiber}$ (tension) = 0.0161
E_{f22} = 15 GPa	$\varepsilon^{ult}_{fiber}$ (compression) = 0.0098
ν_{f12} = 0.28	V_f = 67%
ν_{f23} = 0.19	ε^{ult}_m = 0.0139
G_{f12} = 15 GPa	γ^{ult}_m = 0.06
E_m = 3.2 GPa	σ_y = 48.3 MPa
ν_m = 0.38	----------

the linear portion of measured laminate stress-strain response data. Data from the $[+45°/–45°]_{4S}$ was used to characterize the effective nonlinear stress-strain response of the matrix. To capture matrix failure, the subcell elimination method was used. The subcell elimination method utilizes a user specified failure criterion. After this criterion is satisfied, locally within any of the GMC subcells, all components of the stiffness tensor for that subcell are reduced to a nearly zero value (e.g., 1 percent of original). The criterion employed in this study is based on transverse and shear tensile tests, a strain-based failure criterion with different allowables in tension, ε^{ult}_m and in shear, γ^{ult}_m. Satisfaction of this criterion marks the end of the local matrix stress-strain curve. To capture fiber failure the subcell elimination method was utilized (however, no nonlinearity prior to failure was included in the fiber response), and the allowable was obtained from the unidirectional, [0], coupon test. Table 1 summarizes the complete list of unique model parameters/properties used to calibrate the Plasticity-SE theory. Preliminary results obtained through Tech-Scout I and current results are discussed in the upcoming sections.

Previous prediction results obtained during Tech-scout I program are summarized here. The tensile stiffness prediction matched the experimental result very well with less than 5 percent error for all layups. However, the tensile strength was grossly under predicted by 40.6, 26.3, and 72.8 percent for Layups 1 to 3, respectively. The significant error between the experimentally measured strength and the predicted value for Layup 3 (a shear-dominated composite layup) was the motivation for the present study. The objective is the investigation of the potential causes of this notable difference between simulation and experiment.

As a starting point, the effect of element dimensionality was studied on the obtained FEAMAC solution (Ref. 6); wherein the 3D notched mesh used within this study was reduced to a 2D composite shell mesh (S4R), assuming a macroscopic stress state of plane stress, with the exact same mesh density, boundary conditions and constituent properties (listed in Table 1). Utilization of this 2D composite mesh instead of the prior 3D mesh was motivated by the concept of idealization consistency and resulted in significant improvement in blind (since only the initially characterized model parameters were employed) strength predictions for all three layups. As illustrated in Figure 3, the prediction error relative to ultimate stress was reduced to less than 6 percent for all layups (Figure 3, see green lines), while the relative error for strain to failure was below 25 percent.

Idealization Consistency

Results summarized in Figure 3 prompted the initial assumption that preserving idealization consistency (model dimensionality) throughout characterization to prediction was the driving factor behind the notable difference observed between the 3D and 2D analysis for the above-mentioned layups (especially for Layup 3). However, many interdependent factors are comprised within the concept of idealization consistency and can be classified into three main categories: theoretical, mechanistic and numerical consistencies. Theoretical consistency requires preserving the mathematical aspects (e.g., theory, model dimensionality, functional form, etc.) used throughout characterization to prediction. For example, if the model was characterized using the High fidelity GMC (HFGMC) (Ref. 1) theory, which provides more accurate local stress and strain field predictions than standard GMC, the same theory should be used in subsequent predictions as well, since the associated constitutive model parameters where calibrated assuming this theory. Mechanistic consistency would be associated with assumed measures and definitions of damage and modes of failure and their interactions. For example, if matrix damage or delamination is a

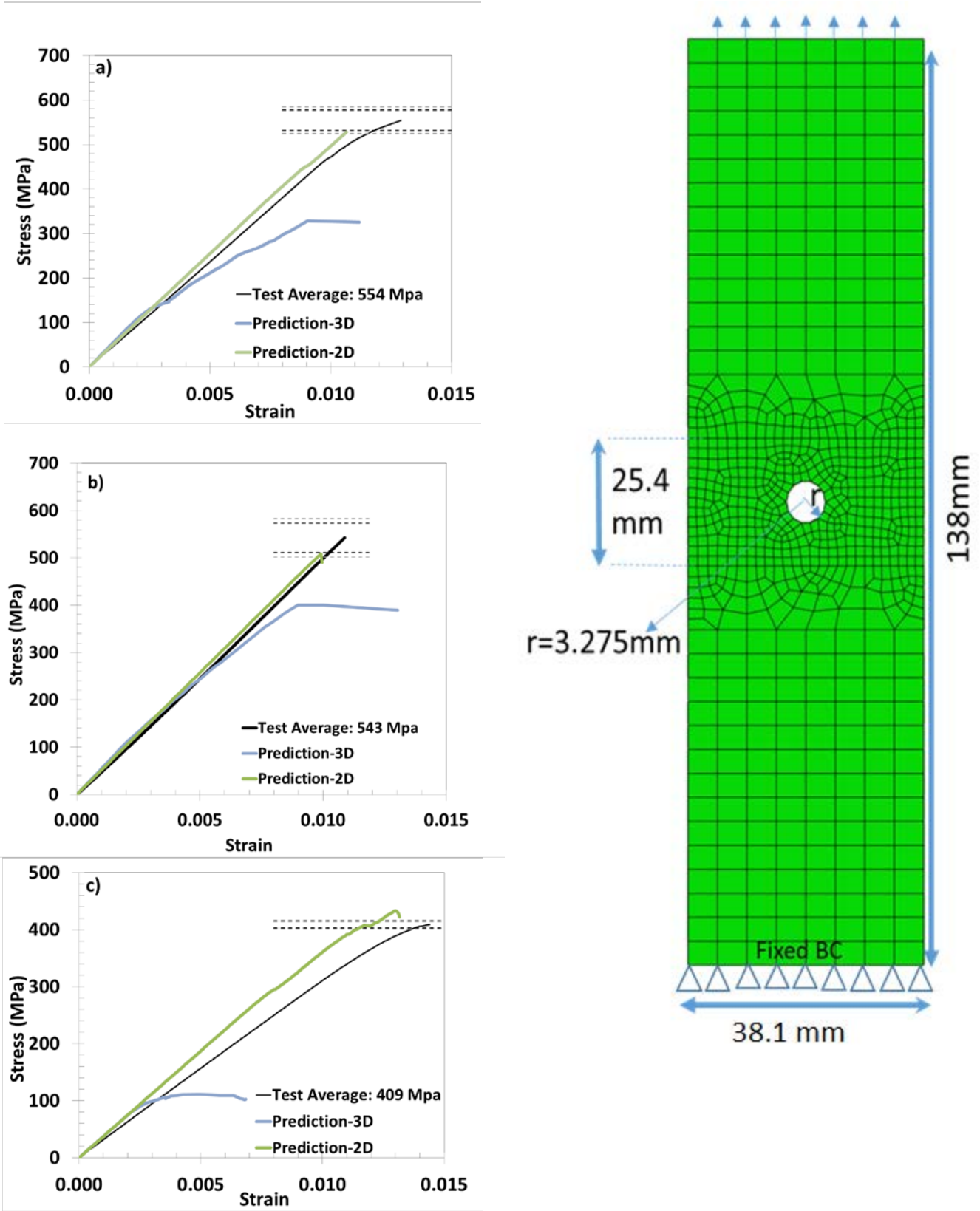

Figure 3.—2D and 3D Blind notched tensile response—FEAMAC/Plasticity-SE, (a) Layup 1: $[0,45,90,–45]_{2S}$, (b) Layup 2: $[60,0,–60]_{3S}$, (c) Layup 3: $[30,60,90,–30,–60]_{2S}$.

major mechanism leading to failure of a laminate, it should be accounted for not only in the final prediction but also during characterization. Length scale (e.g., material volume element) and mesh accuracy are both examples that would fall within the numerical consistency category and thus the preservation of these accuracies from characterization to prediction is important. It is important to remember that these categories are typically not mutually exclusive and thus the influence of one on another is often difficult to explicitly determine. This is particularly true in the case of multiscale analysis wherein all factors can interact aggressively as one traverses length scales. Clearly, at the macro finite element length scale, mesh discretization dependence is a well-known fact; unfortunately, it was not examined during the Tech-Scout I study due to time limitations. In this study, numerical consistency (i.e., mesh dependency) will be a primary focus.

Elastic Solution: Isotropic Plate With Hole

To assess the numerical aspects one needs to clearly understand the distribution of driving forces associated with a given problem. Consequently, the analytical solution of elastic stress fields (in polar coordinates) for a thin, isotropic, infinite plate with a small circular hole under uniaxial tension (Figure 4) (Ref. 7) are considered, see Figure 4.

As observed in Figure 4, stress concentration (or zone of high stress gradient) is quite localized around the hole with a given radius a. Thus, any FE mesh convergence study should focus on the concentration region (marked in Figure 4 with a dashed circle), where $\sigma_{\theta\theta}$ varies from its maximum value to a uniform stress value (σ) within the zone of influence. Setting $\sigma_{\theta\theta} = \sigma$ for a given angular coordinate (θ) in the equation above and solving for radial coordinate (r) provides us with the limit of the concentration region (($\theta = \pi/2$, $r \sim 1.6a$). Based on this simple approximation, a minimum required element size can be estimated, for a given layup, in order to assure the FE model is capable of capturing the high stress gradients around the notch. For the laminates analyzed in Tech Scout I project (a = 3.275), the stress concentration region spans from 3.275 to 5.2 mm and requires a sufficient[1] number of elements need to be placed within this zone to capture this gradient. The mesh convergence study discussed here will be confined to this zone to achieve an objective measure of convergence quality. Since the nonlinear stress gradient profile (see Figure 4) is quadratic in nature a minimum of three points are required in this region, which yields a minimum required element size of ~0.96 mm assuming the use of linear elements and standard integration.

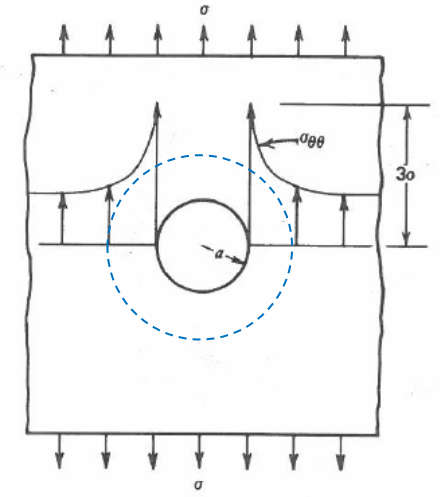

$$\sigma_{rr} = \frac{\sigma}{2}\left(1-\frac{a^2}{r^2}\right)+\frac{\sigma}{2}\left(1-\frac{a^2}{r^2}\right)\left(1-\frac{3a^2}{r^2}\right)\cos 2\theta$$

$$\sigma_{\theta\theta} = \frac{\sigma}{2}\left(1+\frac{a^2}{r^2}\right)-\frac{\sigma}{2}\left(1+\frac{3a^4}{r^4}\right)\cos 2\theta$$

$$\sigma_{r\theta} = -\frac{\sigma}{2}\left(1-\frac{a^2}{r^2}\right)\left(1+\frac{3a^2}{r^2}\right)\sin 2\theta$$

Figure 4.—Elastic stress distribution around the notch.

[1]The order of finite element (i.e., number of integration points) and level of integration (standard or reduced) utilized will clearly influence what constitutes a sufficient number.

Results: Mesh Convergance Study

A closer look into the 3D FEAMAC analysis of Layup 3 ($[30,60,90,-30,-60]_{2S}$) revealed that the matrix subcells in the 90° ply start failing due to extremely large out-of-plane shear strain (ε_{23}) prior to any plastic flow. This early onset of matrix subcell failure in the 3D model leads to faster initiation and growth of plastic flow compared to a corresponding 2D analysis ($\varepsilon^{eq}_{plastic} \sim 0.015$ (3D) and $\varepsilon^{eq}_{plastic} \sim 0.00002$ (2D)), which causes a significant under-prediction of final failure. As mentioned earlier, due to time limitations during the Tech-Scout I project a systematic elastic mesh refinement study was never accomplished. An insufficient mesh was suspected as a potential source of error resulting in the observed significant difference between 2D and 3D analysis, particularly for the Layup 3 case. Therefore, different meshes with increasing mesh densities within the gage section shown in Figure 2 were constructed (see Figure 5) to determine if the observed difference between 3D predictions and experiments stemmed predominantly from an inadequate mesh.

First, an elastic convergence study was conducted to ensure the convergence of elastic fields for all three layups. The 3D FE convergence using the meshes shown in Figure 5 was carried out considering the zone of influence (i.e., concentration region) discussed in the previous section, where all strain components at a given coordinate (marked in Figure 5 by the star) within each laminate layup were recorded for a given off-axis ply. The results are presented in Figure 6. Note that since elastic FE convergence studies are not computationally as expensive as full multiscale analyses, two additional finer mesh densities (0.125 and 0.0625 mm) are added to the ones mentioned in Figure 5 for completeness.

As illustrated in Figure 6 for the case of 3D analysis, all strain components except the transverse shear (ε_{23} for Layup 3) have converged elastically when the element size is 0.5 mm or smaller. The in-plane strains are within 30 percent of the converged case for element size 1mm or less while out-of-plane strains are larger than this for all laminates and in the case of Layup 3 the ε_{23} and ε_{13} are more than a factor of 2 larger. The convergence for the 2D analysis cases are shown in Figure 7 and here it is clear that except for Layup 2 all the in-plane strain components are within 10 percent of the converged mesh results, thus allowing one to reasonably use 1 mm or smaller element size. From these results it is clear that in a 3D analysis one must take extra caution to study convergence rates of out-of-plane strain components, as final failure of some laminates (e.g., soft laminates like Layup 3) might be significantly influenced by these components. In order to have a fully converged strain field, a more conservative element size should be chosen to conduct the computationally intensive multiscale study. Note mesh refinement more than doubles the computational cost from 6 hr (1 mm) to 15 hr (0.5 mm) and then it more than quadruples to 72 hr when moving to a 0.25 mm element size in the case of 3D analyses. In the case of 2D analysis it triples each time, i.e., 1 hr (1 mm), 3 hr (0.5 mm), and 9 hr (0.25 mm). Therefore when desiring to perform multiscale analysis it is important to balance speed with accuracy. However, in the case of 3D analysis, picking a larger element size leads to a nonconverging transverse shear component, which will initiate premature failure (when the failure criterion is based on this component) like in the present case. Consequently, the most probable cause of the significant difference observed between the 2D and 3D open-hole tensile analysis for Layup 3 (Figure 3) is the nonconverging transverse shear strain field for the chosen element size (1 mm).

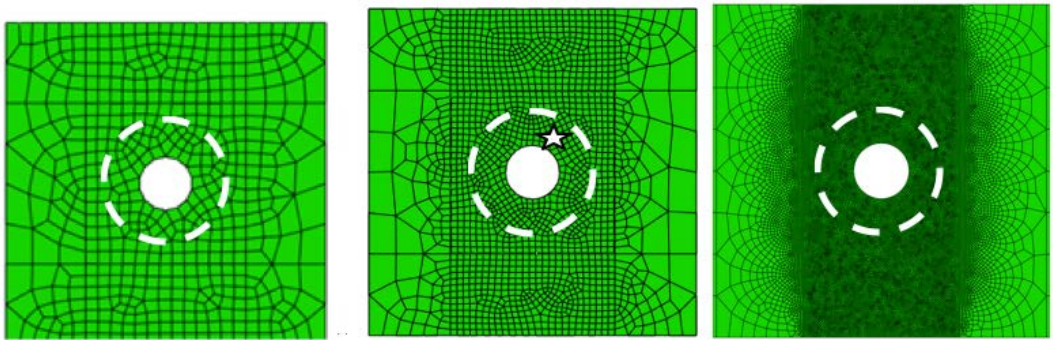

Figure 5.—Snapshot of the meshes in the gage section (left to right: uniform element size: 1, 0.5, and 0.25 mm). Strain readings are recorded at location (x ~73.3 mm, y ~16.5 mm) marked with ☆.

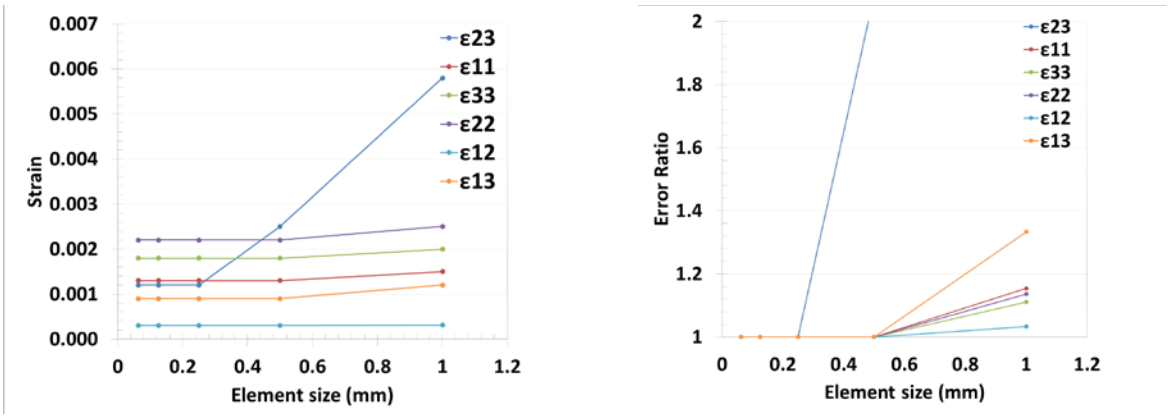

(a) Layup 3, 90° ply

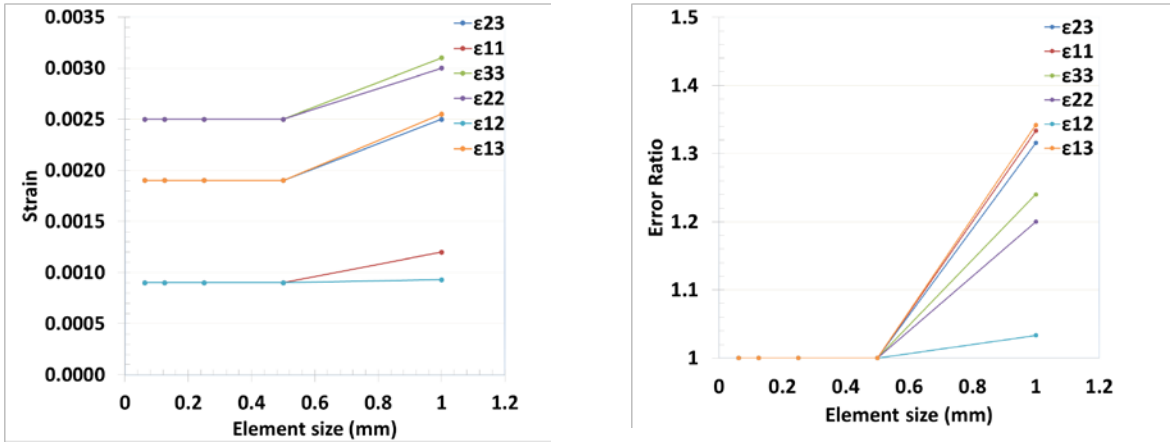

(b) Layup 2, 60° ply

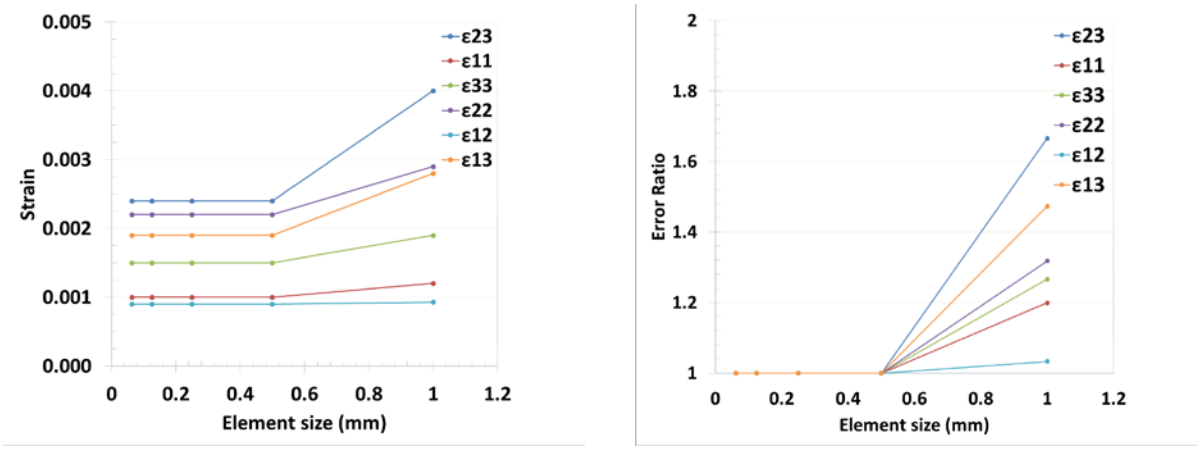

(c) Layup 1, 90° ply

Figure 6.—Elastic strain components and normalized components (error ratio) illustrating convergence of 3D FEA response with respect to different mesh densities.

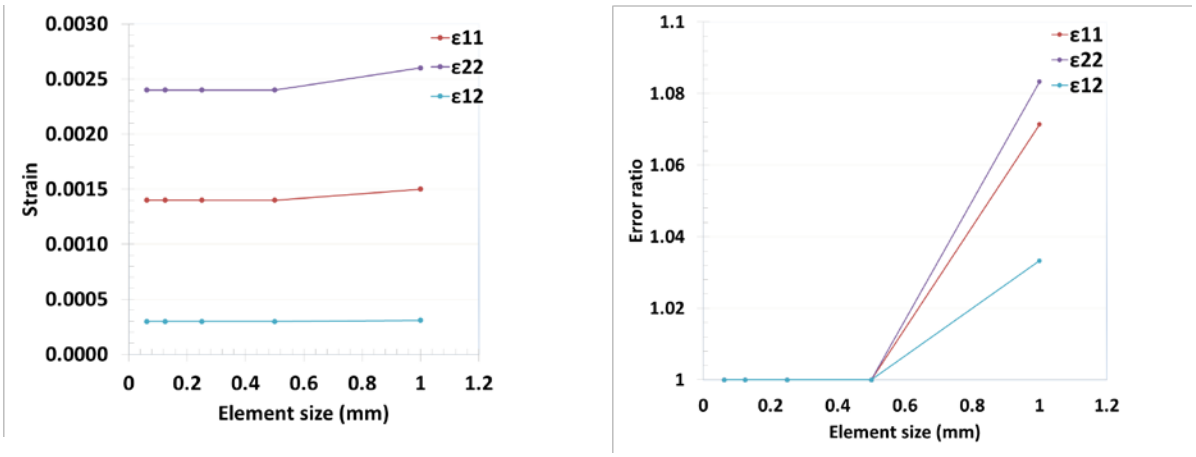

(d) Layup 3, 90° ply

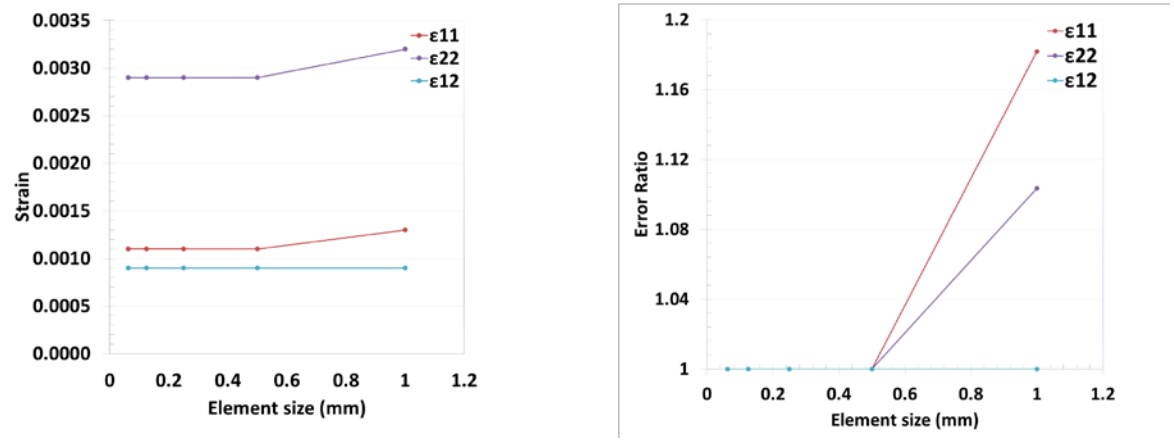

(e) Layup 2, 60° ply

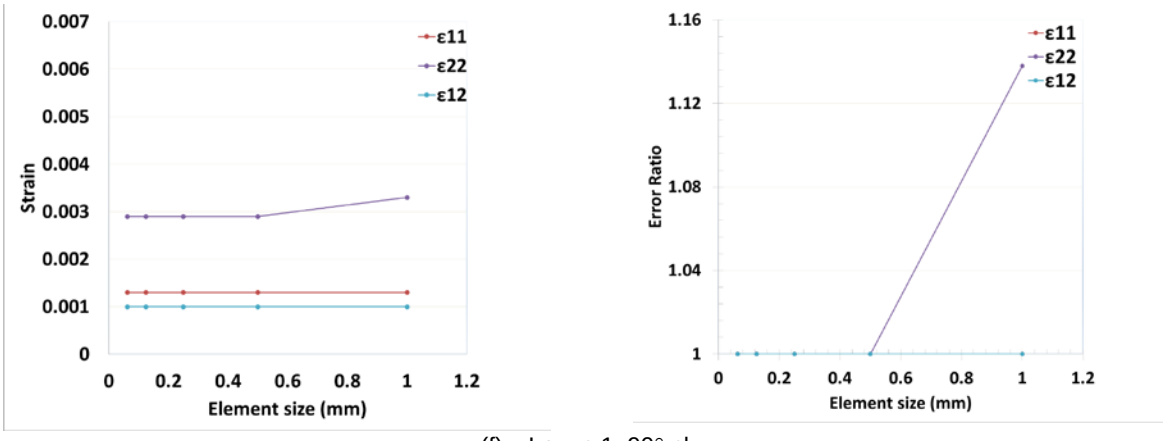

(f) Layup 1, 90° ply

Figure 7.—Elastic strain components and normalized components (error ratio) illustrating convergence of 2D FEA response with respect to different mesh densities.

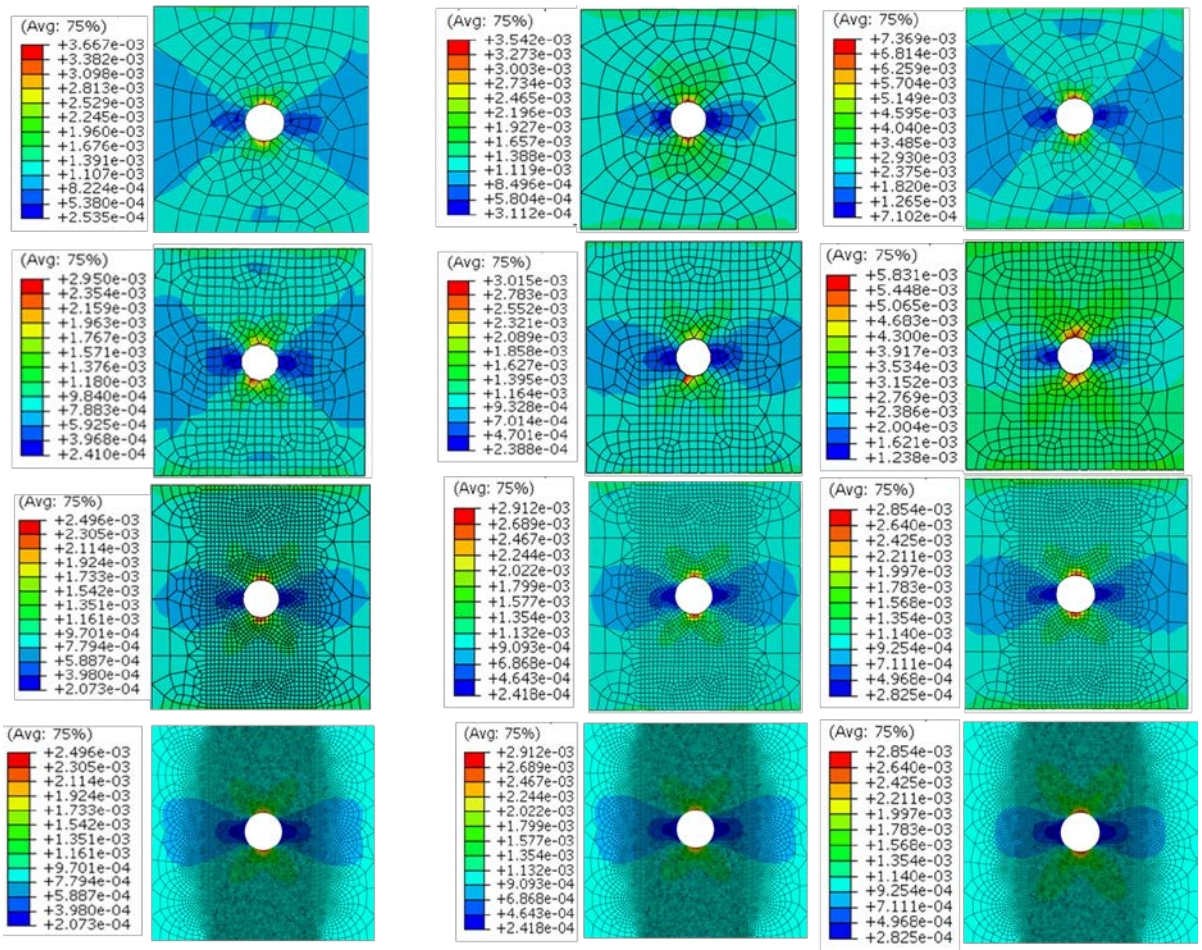

Figure 8.—Contour plots of equivalent elastic strain for Layup 1, Layup 2, and Layup 3 with varying mesh size (top to bottom: 2.5, 1, 0.5, and 0.25 mm).

Figure 6 and Figure 7 dealt with the convergence of strain fields at a given spatial location (identified by the star in Figure 5) within the solutions. Figure 8 illustrates contour plots of the elastic equivalent strain measure over the entire gage area. As shown, a consistent contour pattern for the equivalent elastic strain is developed for all layups when the mesh size is 0.5 mm or below. Similar conclusions can be drawn based on these contour plots as that for a specific location; i.e., reducing element size (from 1 to 0.5 mm and 0.25 mm) reduces the observed difference between the equivalent strain contour plots leading to more accurate final failure estimations.

As illustrated in Figure 9, in-plane refining of the mesh (i.e., reducing element size from 1 to 0.5 mm) reduces the observed difference between a 2D and 3D analysis by approximately 14 percent except in the case of Layup 3 where the difference is 71 percent since the out-of-plane fields have still not converged. Additional mesh refinement (reducing the element size to 0.25 mm) reduces the observed difference between 2D and 3D for Layup 3 to less than 6 percent. Similar trends are observed for the other two layups (Layup 1 and Layup 2) as well, where observed difference between 2D and 3D analysis is lower to less than 6.6 percent with a finer mesh refinement (element size 0.25 mm). Therefore, it can be surmised that insufficient mesh refinement, a form of numerical idealization inconsistency, in 3D analysis led to inaccurate estimations of the through thickness strains, which lead to premature laminate failure initiation especially in shear-dominated laminates (Layup 3 (Ref. 5)). Nevertheless, in laminates containing 0° fibers (Layup 1 and Layup 2 (Ref. 5)) inaccurate through-thickness strain estimations in the 3D model has a less significant impact on final failure because the 0° plies carry the majority of the stress even if the matrix in adjacent plies have completely failed.

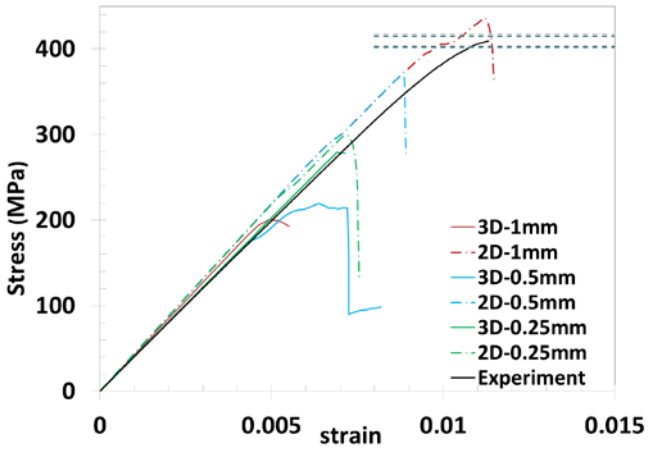

(a) Layup 3

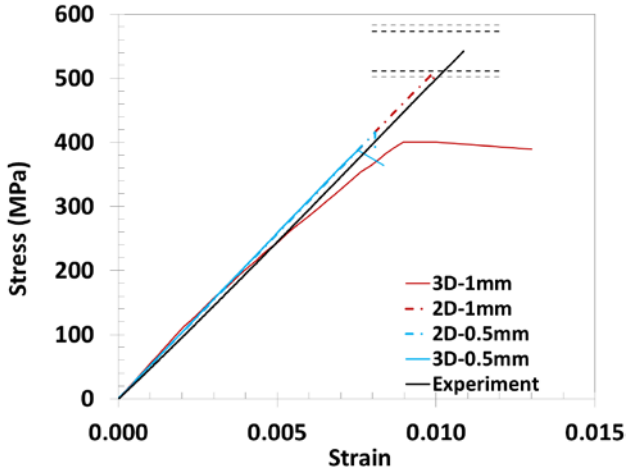

(b) Layup 2

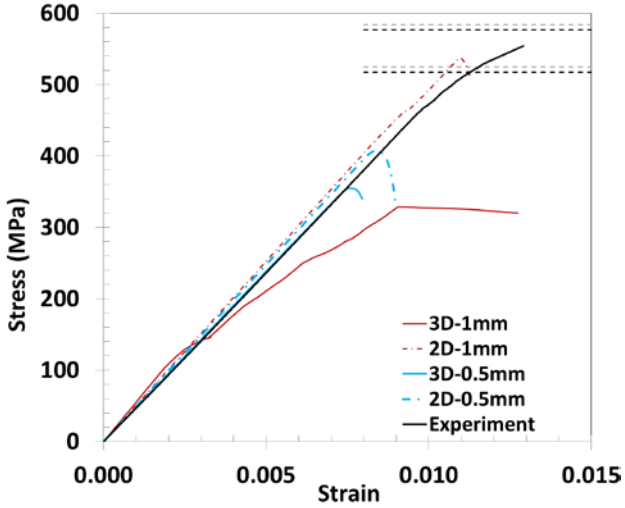

(c) Layup 1

Figure 9.—Open hole tensile response given a 2D and 3D FEAMAC/Plasticity-SE analysis with various uniform mesh densities in the gage section: (1, 0.5, and 0.25 mm).

It is also worth mentioning that since matrix subcell failure is governed by the maximum principal strain criterion in the out-of-plane direction (Table 1: $\varepsilon^{ult}_m = 0.0139$), increasing the specified strain allowable would postpone the failure of the first matrix subcell, and consequently, would prevent the premature failure of the 3D model. This was successfully demonstrated to improve the results during the recalibration phase of the Tech Scout I project (Ref. 6); wherein the ultimate tensile matrix strain allowable (in out-of plane direction) was increased nearly five folds (similar to the error ratio of the out-of-plane shear strains (see Figure 6(a)). This adjustment causes the matrix failure to be circumvented altogether, thus making the 3D methodology approach a 2D one. Consequently, one can see the interdependency of the various idealization consistency factors, in that if one preserves the dimensional (theoretical) consistency the root driving force (out-of-plane shear strains) for the error in simulation is eliminated out right; thus enabling one to get by with a coarser FEA mesh and still obtain reasonable accuracy but with significantly less computational costs. However, to obtain the best answers one must ensure all aspects of idealization consistency (theoretical, mechanistic, and numerical); with numerical (mesh refinement) being a key-driving factor.

Note that the FEAMAC-Plasticity-SE results for static strength predictions are still highly mesh dependent (see Figure 9) because the degradation scheme leads to element volume dependent energy dissipation (Ref. 6). The main focus of this paper is NOT eliminating the overall inherent mesh dependency of the subcell elimination method, but rather investigating the reasons behind the significant difference between 2D and 3D analysis for a given mesh density. As stated in previous work of the authors (Ref. 6), the pathological mesh dependence associated with FEAMAC-Plasticity-SE can be addressed reasonably well by the volume correction method or by utilizing mesh-independent techniques. Here the well-known Weibull volume fraction equation, which was utilized in the previous work of the authors (Ref. 6) (i.e., $\sigma_2/\sigma_1 = (A_1/A_2)^{(1/m)}$, (m = 16)), will be employed to manually adjust the carbon fiber strength for a given finite element volume (i.e., mesh density) so as to minimize this inherent mesh dependent failure behavior. A_1 is the original area assumed for characterization (i.e., the entire gage area of the [0°] unnotched specimen, i.e., $A_1 = 312.5$ mm^2) and A_2 is the area associated with the size of the finite element used in the notched laminate analysis (e.g., 1, 0.25, or 0.0625 mm^2). Results utilizing this modification are shown in Figure 10. Clearly, given a sufficiently converged FE mesh for each Layup and appropriately accounting for the volume ratios very good *predictions*[2] of the open-hole tension problem is obtained for all layups (Layup 3: 12 percent, Layup 2: 9.7 percent, Layup 1: 7.2 percent error compared with experiment). Note that using the above-mentioned weibull equation could lead to unrealistically large fiber strength values for extremely fine meshes and thus should be approached with caution. In the present case of 0.25 mm element size, the calculated fiber strength (7200 MPa) is above the maximum vendor provided fiber strength value of 5700 MPa, but still significantly below that of single crystal graphite; thus this value is deemed reasonable.

Similar to Tech-Scout I project (Ref. 6) minor modifications can be made to recalibrate and further improve the reported *predictions*[2] (weibull correction plots) in Figure 10. For example, increasing matrix failure strain (ε^{ult}_m) by roughly 50 percent (from $\varepsilon^{ult}_m = 0.0139$ to 0.02) and decreasing fiber stiffness by 10 percent (from 276 GPa to 250 GPa) leads to a better estimation of the measured maximum strength and overall stiffness for all layups (see Figure 11). The recalibration results fall within the measured error band of the experiments themselves; ±5.6 percent.

Note that the overall average difference in strength prediction reported in the Tech-Scout Project I (Ref. 5) (considering all reported methods) would also decrease from 18.7 percent to approximately 16.8 percent if we replace our original error values with those from the current study. Additional improvement in the other overall averages is expected by further minimizing the error for open-hole compression and un-notched specimens through improving mesh consistency and following the modifications suggested in this paper.

[2]These simulations could be considered blind predictions since all model parameters used are those associated with those obtained during the original characterization of the models.

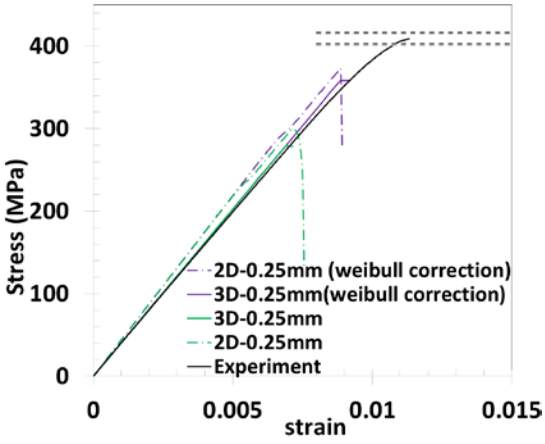

(a) Layup 3

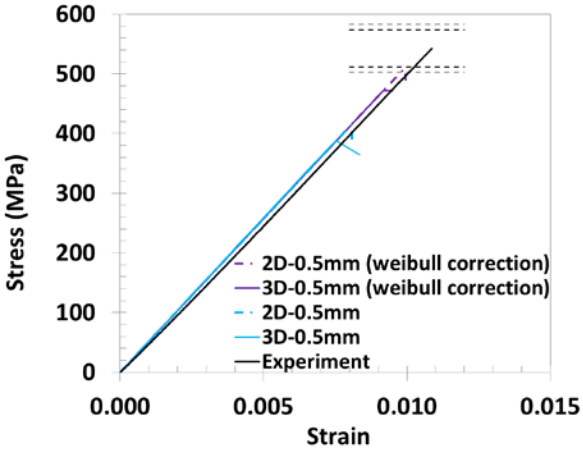

(b) Layup 2

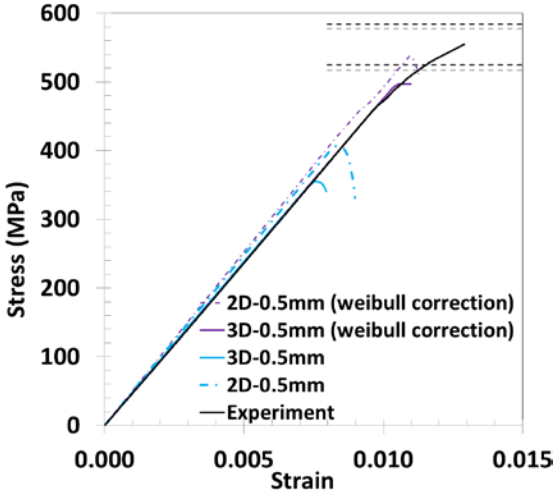

(c) Layup 1

Figure 10.—Open hole tensile response given a 2D and 3D FEAMAC/Plasticity-SE analysis with a converged uniform mesh in the gage section (Layup 1 and Layup 2: 0.5 mm, Layup 3: 0.25 mm) and weibull correction.

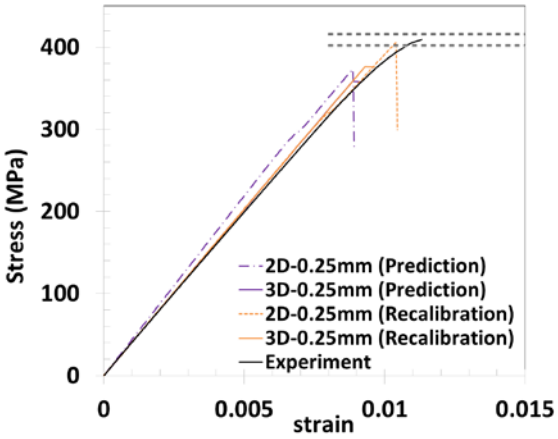

(a) Layup 3

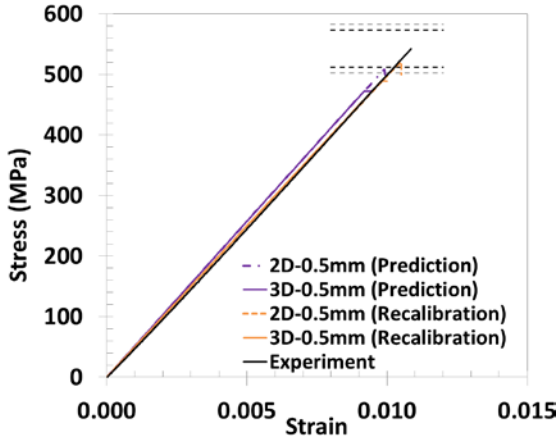

(b) Layup 2

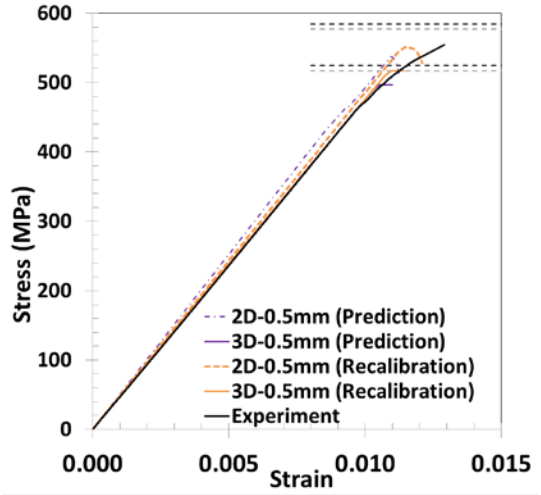

(c) Layup 1

Figure 11.—Recalibration of an open hole tensile response using a 2D and 3D FEAMAC/Plasticity-SE analysis with a converged uniform mesh in the gage section (Layup 1 and Layup 2: 0.5 mm, Layup 3: 0.25 mm).

Conclusions

In this paper, the open-hole tensile simulations from a recent AFRL Tech-Scout program are revisited. The results presented demonstrate the criticality of performing an elastic FE mesh convergence study prior to conducting any failure predictions. It was also shown that the out-of-plane shear stress was the primary source of the difference between 3D and 2D analyses when insufficient mesh refinement is allowed to exist. Further, the observed difference between 2D and 3D results was significantly improved by refining the mesh along in-plane directions (especially for Layup 3), although the computational cost of a 3D analysis far exceeded that of a 2D analysis. Consequently, although a 3D analysis is normally considered to be a more realistic representation of experiments, it should be avoided unless sufficient mesh refinement (both in-plane and/or out-of-plane) and adequate computational resources are available. Therefore we recommend employment of 2D continuum shell elements whenever possible (e.g., when delamination can be ignored) and particularly when conducting computationally demanding multiscale analyses (e.g., micromechanics-based FE analyses).

It was unfortunate that a thorough mesh convergence study was not done during the Tech-Scout I project timeline, since our ability to make accurate blind predictions was greatly impacted. As evidenced in this paper, improving numerical consistency and following the minor modifications/improvements in constituent properties resulted in MAC/GMC predictions within the experimental variability of ±5.6 percent.

References

1. Aboudi, J., Arnold, S.M., and Bednarcyk, B.A. (2013) Micromechanics of Composite Materials: A Generalized Multiscale Analysis Approach, Elsevier, Oxford, UK.
2. Dassault Systèmes Simulia Corp. (2011): Abaqus User's Manual, Vol. 1–3, Version 6.11-1. Dassault Systèmes Simulia Corp., Providence, RI, 2011.
3. Qizhou Yao and Jianmin Qu. (1999): Three-dimensional vs. two-dimensional finite element modeling of flip chip packages. Journal of Electronic Packaging, Transactions of the ASME;121(3):196–201.
4. Krueger R., Paris Isabelle L., and O'Brien Kevin. (2002) Comparison of 2D finite element modeling assumptions with results from 3D analysis for composite skin-stiffener debonding. Composite Structures. Volume 57, Issues 1–4, Pages 161–168.
5. Engelstad, S.P., Action, J.E., Clay, S.B., Holzwarth, R.C., Robbins, D., Dalgamo, R. (2015) Assessment of composite damage growth tools for aircraft structure part I. *AIAA Science and Technology Forum, 56th AIAA/ASCE/AHS/ASC Structures, Structural Dynamics, and Materials Conference*. 5–9 January, Kissimmee, Florida.
6. Naghipour P., Arnold S.M., Pineda E.J., Stier B., Hansen L., Bednarcyk B.A., Waas A.M. (2016), Multiscale Static Analysis of Notched and Un-notched Laminates using the Generalized Method of Cells. To appear Journal of Composite Materials. DOI: 10.1177/0021998316651708.
7. Landau L.D., Pitaevskii L.P., Kosevich A.M. and Lifshitz E.M. (1986) Theory of Elasticity, 3rd edition, Volume 7 (Course of Theoretical Physics). Butterworth-Heinemann.